Atmos. Chem. Phys., 24, 11717–11725, 2024
https://doi.org/10.5194/acp-24-11717-2024

Atmospheric Chemistry and Physics
Open Access
EGU

Predicting hygroscopic growth of organosulfur aerosol particles using COSMOtherm

Zijun Li[1], Angela Buchholz[2], and Noora Hyttinen[3,a]

[1]International Laboratory for Air Quality and Health, School of Earth and Atmospheric Sciences, Queensland University of Technology, Brisbane, QLD 4001, Australia
[2]Department of Technical Physics, University of Eastern Finland, Kuopio 70210, Finland
[3]Department of Chemistry, Nanoscience Center, University of Jyväskylä, Jyväskylä 40014, Finland
[a]now at: Atmospheric Research Centre of Eastern Finland, Finnish Meteorological Institute, Kuopio 70211, Finland

Correspondence: Zijun Li (zijun.li@qut.edu.au) and Noora Hyttinen (noora.hyttinen@fmi.fi)

Received: 20 April 2024 – Discussion started: 7 May 2024
Revised: 12 July 2024 – Accepted: 3 September 2024 – Published: 21 October 2024

Abstract. Organosulfur (OS) compounds are important sulfur species in atmospheric aerosol particles, due to the reduction of global inorganic sulfur emissions. Understanding the physicochemical properties, such as hygroscopicity, of OS compounds is important for predicting future aerosol–cloud–climate interactions. However, their hygroscopicity is not yet well understood due to the scarcity of authentic standards. In this work, we investigated a group of OS compounds with short carbon chains (C_1–C_5) and oxygen-containing functional groups in the form of sodium, potassium, or ammonium salts and their mixtures with ammonium sulfate. The hygroscopic growth factors (HGFs) of these OS compounds have been experimentally studied. Here, the HGFs were calculated from mass fraction of water that was computed using the conductor-like screening model for real solvents (COSMO-RS). A good agreement was found between the model-estimated and experimental HGFs for the studied OS compounds. This quantum-chemistry-based approach for HGF estimation will open up the possibility of investigating the hygroscopicity of other OS compounds present in the atmosphere.

1 Introduction

Atmospheric aerosol particles affect the global climate directly by scattering solar radiation or indirectly by seeding clouds. As important aerosol constituents, organosulfur (OS) compounds contribute up to 30 % of total organic aerosol particles in mass (Surratt et al., 2008; Tolocka and Turpin, 2012). Typically, these OS compounds contain a sulfonate or sulfate ester group. Methanesulfonic acid, the most abundant OS compound in marine environments, can be produced via both gas-phase and aqueous-phase oxidation of reduced-sulfur compounds (Barnes et al., 2006; Hoffmann et al., 2016; Berndt et al., 2023). Another OS compound of high abundance (Moch et al., 2020), namely hydroxymethanesulfonate, is formed from sulfite and formaldehyde in the aqueous phase (Boyce and Hoffmann, 1984; Song et al., 2019). Moreover, other OS compounds can be formed via multiphase oxidation of biogenic as well as anthropogenic organic compounds in the presence of sulfuric acid. To date, OS compounds have been identified in various environments across forest (Iinuma et al., 2007; Kristensen and Glasius, 2011), coastal (Huang et al., 2015; Zhou et al., 2023), polar (Hansen et al., 2014; Ye et al., 2019; Campbell et al., 2022), and urban sites (Jiang et al., 2022; Glasius et al., 2022). Therefore, the abundance and ubiquity of OS compounds in the atmosphere highlight their importance for global climate.

Understanding the interactions of OS compounds with water vapor as a function of relative humidity (RH) is important in assessing their climate effect. When in equilibrium with surrounding RH, the degree of water uptake (i.e., hygroscopicity) largely affects aerosol phase states, optical properties, chemical reactivity, and cloud formation potential. A range

of laboratory studies have investigated the hygroscopicity for both commercially available and synthesized OS compounds under subsaturated (RH < 100 %) conditions (Hansen et al., 2015; Estillore et al., 2016; Peng et al., 2021, 2022; Ohno et al., 2022; Bain et al., 2023). Inorganic salts typically show distinct deliquescence and efflorescence RH (DRH and ERH, respectively) points, while the studied OS compounds consistently show continuous growth with increasing RH. Furthermore, the presence of OS compounds can lower the DRH and ERH of inorganic salt particles (Estillore et al., 2016; Peng et al., 2021, 2022) and potentially extends the RH range where particulate water is present, thus influencing the physicochemical properties of atmospheric aerosol particles.

Both Aerosol Inorganic–Organic Mixtures Functional Groups Activity Coefficients (AIOMFAC) (Zuend et al., 2008, 2011; Zuend and Seinfeld, 2012) and the conductor-like screening model for real solvents (COSMO-RS) (Klamt, 1995; Klamt et al., 1998; Eckert and Klamt, 2002) can estimate the activity coefficients of compounds present in atmospheric aerosol particles as a function of RH. Previous thermodynamic studies have shown that both AIOMFAC and COSMO-RS can provide similar predicted water activities (α_w) in aqueous $(NH_4)_2SO_4$, NH_4HSO_4, NH_4NO_3, and NH_4IO_3 (Hyttinen, 2023a), as well as in carboxylic acids (Hyttinen et al., 2020b; Hyttinen and Prisle, 2020). The group contribution calculations in AIOMFAC can be finished in seconds, while the quantum chemistry calculations in COSMO-RS require hours to be completed. However, COSMO-RS is the only existing method able to estimate α_w in OS solutions. Recently, the solubilities and activities of isoprene- and monoterpene-derived organosulfates were computed using COSMO-RS (Hyttinen et al., 2020a). To our knowledge, there is, however, no comparison between the experimental and thermodynamic model-estimated hygroscopicity of OS compounds, which become increasingly important due to declining SO_2 emissions (Riva et al., 2019). This hinders the understanding of their atmospheric impacts and fates.

Here, we perform quantum chemistry calculations with COSMO-RS to explore a set of atmospherically relevant OS compounds (Table S1 in the Supplement):

- Sodium OS includes methyl sulfate (NaMS), hydroxymethanesulfonate (NaHMS), ethyl sulfate (NaES), and 2-hydroxyethyl sulfonate (NaHES).

- Potassium OS includes glycolic acid sulfate (KGAS), hydroxyacetone sulfate (KHAS), 2-butenediol sulfate (KBS), and 4-hydroxy-2,3-epoxybutane sulfate (KHEBS).

- Ammonium OS includes 2-hydroxyethyl-sulfonate (NH_4HES), (2R,3S)-1,3,4-trihydroxy-2-methylbutan-2-yl sulfate (NH_4TMS (a)), and (2R,3R)-2,3,4-trihydroxy-2-methylbutan-2-yl sulfate (NH_4TMS (b)).

The experimental hygroscopicities of these OS compounds are reported in the literature (Estillore et al., 2016; Peng et al., 2021, 2022; Ohno et al., 2022). For each studied OS compound, we estimate the corresponding α_w at a range of solute concentrations to predict the hygroscopic growth curves. Additionally, we predict particle hygroscopicity for the OS mixed with ammonium sulfate (AS; $(NH_4)_2SO_4$), which is the most abundant inorganic salt in atmospheric aerosol particles.

2 Computational methods

2.1 Activity coefficients

The COSMO-RS model (Klamt, 1995; Klamt et al., 1998; Eckert and Klamt, 2002), implemented in the BIOVIA COSMOtherm program (BIOVIA COSMOtherm, 2021) (abbreviated COSMOtherm), was used to calculate activity coefficients of water under vapor–liquid equilibrium. All activity coefficients were calculated using the BP_TZVPD_FINE_21 parameterization (abbreviated FINE), with the exception of solutions containing AS, which were calculated using the newly developed electrolyte parameterization BP_TZVP_ELYTE_21 (abbreviated ELYTE; see Sect. S1 in the Supplement for more details). The activity coefficient γ_j of a compound j is computed using the pseudo-chemical potential μ^* (Ben-Naim, 1987) at composition $\boldsymbol{x}$ and at the reference state $\boldsymbol{x}^\circ$:

$$\ln \gamma_j(\boldsymbol{x}) = \frac{\mu_j^*(\boldsymbol{x}) - \mu_j^{*,\circ}(\boldsymbol{x}^\circ, T, P)}{RT}, \quad (1)$$

where T is the temperature (295 K), R is the gas constant (in kJ K^{-1} mol^{-1}), and $P = 10^5$ Pa is the reference pressure. The pseudo-chemical potential μ_j^* is an auxiliary quantity defined using the chemical potential at the reference state μ°:

$$\mu_j^*(\boldsymbol{x}) = \mu_j{}^\circ(\boldsymbol{x}^\circ, T, P) + RT \ln \gamma_j(\boldsymbol{x}). \quad (2)$$

Pure water with a mole fraction (x_w) of 1 is used as the reference state composition $\boldsymbol{x}^\circ$. With the calculated γ_j, each aqueous-phase composition is paired with a RH assuming that, at equilibrium, $\alpha_w = \mathrm{RH}/100\,\%$, where $\alpha_w = x_w \gamma_w$.

2.2 Input files for COSMOtherm calculations

Input files for COSMOtherm calculations (COSMO files) were obtained through a series of density functional theory calculations with increasing levels of theory. The process has been discussed in more detail in a previous publication (Hyttinen et al., 2020a). In short, all conformers were found using the systematic conformer search algorithm in the Spartan20 program (Wavefunction Inc., 2020). The geometries of all conformers were optimized, and duplicate conformers were removed using the BIOVIA COSMOconf program (BIOVIA COSMOconf, 2021; TURBOMOLE, 2020).

The final COSMO files were computed at the BP/def2-TZVPD-FINE//BP/def-TZVP level of theory (BP/def-TZVP for BP_TZVP_ELYTE_21 calculations).

Many of the studied anions have multiple conformers. At most 10 lowest chemical potential conformers were selected as inputs for the COSMOtherm calculations. However, only conformers with chemical potentials within 8 kJ mol^{-1} of the lowest chemical potential were used, in order to avoid including conformers with low COSMO energies but high chemical potentials (Hyttinen, 2023b). More specifically, COSMOtherm gives high weights to conformers containing intramolecular H-bonds (Hyttinen and Prisle, 2020), because intramolecular H-bonds are favored in the COSMO energies (Kurtén et al., 2018).

2.3 Predicting HGF of OS particles

The hygroscopicity of an organic compound is typically quantified using the hygroscopic growth factor (HGF), which is the ratio of the diameter under a RH condition i ($D_{p,i}$) to the diameter under dry conditions (RH≤10 %; $D_{p,0}$):

$$\mathrm{HGF} = \frac{D_{p,i}}{D_{p,0}}. \tag{3}$$

Assuming particle sphericity, HGF can be further expressed by

$$\mathrm{HGF} = \left(\frac{V_{p,i}}{V_{p,0}}\right)^{\frac{1}{3}}, \tag{4}$$

where $V_{p,i}$ and $V_{p,0}$ are the particle volumes under a RH condition i and dry conditions, respectively. Assuming volume additivity, HGF can be represented using the volume of water and the solute (V_{OS} and V_{H_2O}).

$$\mathrm{HGF} = \left(\frac{V_{OS} + V_{H_2O,i}}{V_{OS} + V_{H_2O,0}}\right)^{\frac{1}{3}} \tag{5}$$

The volume of each component j (V_j) can be written using the mass at RH = i ($m_{j,i}$) and density ρ_j:

$$V_j = \frac{m_{j,i}}{\rho_j}. \tag{6}$$

In COSMOtherm, ρ_j is estimated from the molecular volumes of individual species present in the mixture, assuming close packing. Therefore, the formation of intermolecular H-bonds within the mixture is not considered in the density calculation.

Combing Eqs. (5) and (6) leads to

$$\mathrm{HGF} = \left(\frac{\frac{m_{OS}}{\rho_{OS}} + \frac{m_{H_2O,i}}{\rho_{H_2O}}}{\frac{m_{OS}}{\rho_{OS}} + \frac{m_{H_2O,0}}{\rho_{H_2O}}}\right)^{\frac{1}{3}} = \left(\frac{1 + \frac{m_{H_2O,i}\cdot\rho_{OS}}{m_{OS}\cdot\rho_{H_2O}}}{1 + \frac{m_{H_2O,0}\cdot\rho_{OS}}{m_{OS}\cdot\rho_{H_2O}}}\right)^{\frac{1}{3}}, \tag{7}$$

where the mass ratio between m_{H_2O} and m_{OS} can be predicted using the COSMOtherm-estimated mass fraction of water at equilibrium. This approach treats the OS particles as a bulk phase without considering particle size.

2.4 Predicting HGF of OS–AS mixture particles

COSMOtherm calculations assume that all salts are dissolved in water regardless of the water content. However, AS may not fully dissolve in aqueous mixtures under low RH conditions. Previous experimental studies have shown that when AS is mixed with certain carboxylic acids (Choi and Chan, 2002; Chan et al., 2006) and OS (Peng et al., 2021, 2022), a step change in HGF was typically observed at or below the DRH of AS, which is attributed to the full dissolution of AS. In other words, at RH below the observed step change in HGF, AS may exist in a crystalline solid state or partially dissolve in the liquid phase. For all the studied OS–AS mixture particles, stepwise changes in HGFs were observed in the measurements conducted by Peng et al. (2021, 2022). Similar to Hodas et al. (2016), who studied the HGF of polyethylene glycol oligomers mixed with AS, we assume that AS exists only in the solid state before reaching full deliquescence in the calculations. When the RH increases above the DRH, AS reaches its solubility limit and undergoes a solid-to-liquid phase transition. At the DRH, the molar ion activity product (IAP) of the inorganic salt (e.g., AS) will be the same, regardless of other components in the mixture. It is therefore possible to determine the DRH of different salt mixtures if the IAP of the inorganic salt for one saturated solution ($\mathrm{IAP_{sat}}$) can be calculated.

For a specific ion, the molal activity coefficient $\gamma_{j,b}$ can be computed using the mole-fraction-based activity coefficient $\gamma_{j,x}$ estimated by COSMOtherm (Robinson and Stokes, 2002):

$$\gamma_{j,b} = \frac{\gamma_{j,x}}{1 + 0.001 \cdot \mathrm{MW} \cdot \Sigma_j \nu_j b_j}, \tag{8}$$

where MW is the molar mass of the solvent water, ν_j is the number of moles of ions formed by the ionization of one mole of salt j (three for AS and two for OS), and b_j is the molality (i.e., moles of solute per kilogram of water) of salt j. The IAP of AS in a solution can be calculated using the molal ionic activity coefficients and molalities of NH_4^+ and SO_4^{2-} (Robinson and Stokes, 2002):

$$\mathrm{IAP} = \left[\gamma_{NH_4^+,b} \cdot b_{NH_4^+}\right]^2 \left[\gamma_{SO_4^{2-},b} \cdot b_{SO_4^{2-}}\right]^1. \tag{9}$$

The $\mathrm{IAP_{sat}}$ is calculated using the aqueous solubility limit of AS (i.e., 5.790 mol AS per kilogram of water at 295 K). When the estimated IAP > $\mathrm{IAP_{sat}}$, AS is assumed to exist only in its solid form. In this case, the OS is the sole component contributing to the particle water uptake. Under such a condition, we apply the Zdanovskii–Stokes–Robinson (ZSR) approach (Stokes and Robinson, 1966) to estimate the particle water uptake, assuming no interactions between AS and the liquid phase. The corresponding HGF of the OS–AS mixture is derived by multiplying the COSMOtherm-estimated HGF for the pure OS with the OS volume fraction in the OS–AS mixture. When the estimated IAP ≤ $\mathrm{IAP_{sat}}$, AS is

assumed to be fully dissolved in the liquid phase and well mixed with OS. Similar to Eq. (7), which treats the particles as a bulk phase, the HGF in this case can be derived based on the COSMOtherm-estimated mass fraction of water of the OS–AS mixture, with the aid of Eq. (10):

$$\mathrm{HGF} = \left(\frac{\frac{m_{\mathrm{OS}}}{\rho_{\mathrm{OS}}} + \frac{m_{\mathrm{AS}}}{\rho_{\mathrm{AS}}} + \frac{m_{\mathrm{H_2O},i}}{\rho_{\mathrm{H_2O}}}}{\frac{m_{\mathrm{OS}}}{\rho_{\mathrm{OS}}} + \frac{m_{\mathrm{AS}}}{\rho_{\mathrm{AS}}} + \frac{m_{\mathrm{H_2O},0}}{\rho_{\mathrm{H_2O}}}} \right)^{\frac{1}{3}} = \left(\frac{1 + \frac{m_{\mathrm{AS}} \cdot \rho_{\mathrm{OS}}}{m_{\mathrm{OS}} \cdot \rho_{\mathrm{AS}}} + \frac{m_{\mathrm{H_2O},i} \cdot \rho_{\mathrm{OS}}}{m_{\mathrm{OS}} \cdot \rho_{\mathrm{H_2O}}}}{1 + \frac{m_{\mathrm{AS}} \cdot \rho_{\mathrm{OS}}}{m_{\mathrm{OS}} \cdot \rho_{\mathrm{AS}}} + \frac{m_{\mathrm{H_2O},0} \cdot \rho_{\mathrm{OS}}}{m_{\mathrm{OS}} \cdot \rho_{\mathrm{H_2O}}}} \right)^{\frac{1}{3}}, \quad (10)$$

where m_{AS} and ρ_{AS} are the mass and density of AS, respectively.

3 Results and discussion

3.1 Water activity of OS

Water activity of the studied OS was estimated in solutions with water mass fractions (m_{w}) ranging from 0 to 0.96 (Fig. 1). Since different OS compounds have different molecular weights, using m_{w} enables a direct comparison of the water uptake for the studied salts. All OS compounds are assumed to be fully dissolved in the water as ions. Due to the scarcity of experimental data on α_{w} for the studied OS, it is not possible to determine the relative errors of the model estimates for all studied OS. Compared with the only existing measured α_{w} data from Bain et al. (2023), COSMOtherm calculations provided similar values of α_{w} for NaMS and NaES (Fig. S2 in the Supplement).

In the sodium OS group, the studied OS compounds with the same carbon number exhibit higher m_{w} with more oxygenated functional groups at a fixed α_{w} below 0.7 (i.e., RH below 70 %). Here, COSMOtherm predicts higher α_{w} in more concentrated solutions and lower α_{w} in more diluted solutions for NaMS and NaES, compared to those containing the isomeric hydroxy sulfonate salts (i.e., NaHMS and NaHES). This is likely caused by the relatively more hydrophobic nature of the methyl and ethyl groups compared to anions that contain hydrogen-bond-donating functional groups (e.g., −OH groups). Similar but stronger patterns in α_{w} are seen in the unstable regions of phase-separating mixtures (Hyttinen, 2023b). In the potassium OS group, the selected OS compounds display higher m_{w} with increasing molecular weights at a fixed α_{w}. The three chosen ammonium OS compounds show similar degrees of water uptake, independent of the anion. When comparing the three cation groups (i.e., Na^+, K^+, and NH_4^+), we observed that at a fixed α_{w}, the group of potassium OS (Fig. 1b) shows the lowest degree of water uptake, as indicated by the lowest m_{w}. Note that most of the anions are different between the three cation groups. The difference in α_{w} between the three cation groups can arise from the differences in cations and/or anions.

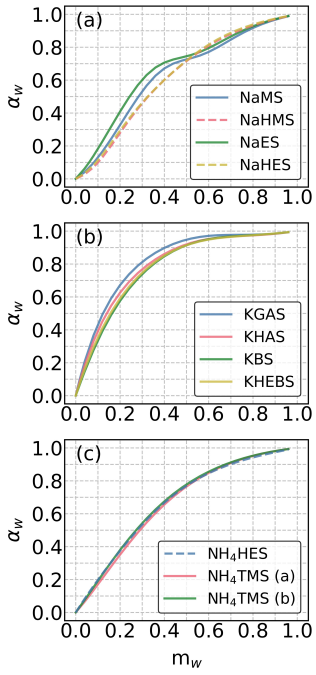

Figure 1. COSMOtherm-derived water activities (α_{w}) in aqueous solutions of the studied **(a)** sodium, **(b)** potassium, **(c)** and ammonium OS as a function of water mass fraction (m_{w}) at 295 K. The solid and dashed lines represent salts of organosulfates and organosulfonates, respectively.

To rule out the effect of cations, we additionally computed the α_{w} for all cation–anion pairs (Fig. S3). Regardless of the anion, at any α_{w}, potassium OS compounds show the lowest m_{w}, as compared to the corresponding sodium and ammonium OS. Note that at $\alpha_{\mathrm{w}} \leq 0.7$, most sodium OS compounds have lower equilibrium water content compared to the corresponding ammonium OS. However, at $\alpha_{\mathrm{w}} > 0.7$, both sodium and ammonium OS compounds show similar equilibrium water content for each of the studied anions. Moreover, for each studied OS, the order of cations is more or less the same, suggesting the presence of the Hofmeister effect. Sodium is usually enriched in sea spray particles (Salter et al., 2016), while potassium and ammonium are commonly found in continental aerosol particles influenced by biomass burning (Vasilakopoulou et al., 2023) and anthropogenic ammonia sources (Pai et al., 2021). Therefore, the α_{w} of OS in aerosol particles may vary depending on the influence of marine and continental air masses.

3.2 Hygroscopicity of OS particles

We calculated the HGF for each studied OS, on the basis of the COSMOtherm-estimated m_{w} and density (ρ, Table S1). The corresponding COSMOtherm-estimated HGFs with the experimental data are shown for three selected OS (i.e., NaMS, KGAS, and NH_4HES) particles in Fig. 2. Both the measured and computed HGFs are very similar to each other.

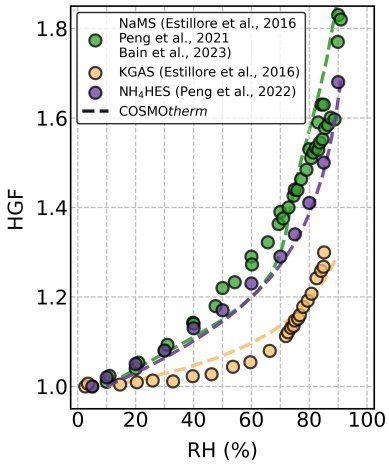

Figure 2. Hygroscopic growth factors (HGFs) for sodium methyl sulfate (NaMS; green), potassium glycolic acid sulfate (KGAS; yellow), and ammonium 2-hydroxyethyl-sulfonate (NH_4HES; purple) as a function of RH at 295 K. The HGF data from the literature (Estillore et al., 2016; Peng et al., 2021, 2022; Bain et al., 2023) and the COSMOtherm-derived calculations are shown with solid circles and dashed lines, respectively.

Figure S4 summarizes the experimental and computed HGF data of all the studied OS particles as a function of RH. To evaluate the model performance for the studied OS particles, we compared the model simulations against the measurement data as indicated by the relative differences shown in Fig. S5. There are different possible sources of uncertainties that may explain the discrepancy between experimental data and COSMOtherm estimates. The uncertainty can originate from the errors in the experiments, the COSMOtherm-estimated α_w, or the assumptions made for calculating the HGF from m_w. In this study, most of the discrepancies likely originate from the COSMOtherm-estimated α_w of some of the ions. The original COSMOtherm parameterization (Klamt et al., 1998) provided only poor estimates for water. The FINE parameterization performs much better, and we found relatively good agreement between experimental data and our HGF calculations. Note that the COSMOtherm-predicted HGFs overall agree very well with the measurement data, mostly showing relative differences of $\pm 5\,\%$ or less compared to the measured HGFs (Fig. S5). This agreement highlights the validation of using m_w and ρ from COSMOtherm to predict the hygroscopic growth of OS particles.

In addition, we compared the HGF data using all three available parameterizations of the COSMO*therm* program (FINE, TZVP, and ELYTE), as shown in Fig. S6. For the four studied sodium OS particles, ELYTE gave similarly good or even better HGF estimates than FINE. For the potassium OS particles, the FINE HGF estimates show the best agreement with the measurement data, compared to the TZVP and ELYTE estimates. When considering the three studied ammonium OS particles, the three parameterizations provided similar RH dependency of HGFs but gave only reasonably good HGF estimates for NH_4HES particles. Among the three COSMOtherm parameterizations, FINE overall provided the best agreement across all the studied OS particles and showed the smallest relative differences compared to the measurement data (Fig. S5). Therefore, FINE was chosen for the detailed analysis here.

We acknowledge that the effect of surface tension was not taken into account in the HGF calculation for each studied OS. However, considering the dry OS particle size of 100 nm or larger from the experimental studies, the surface tension effect can be assumed to be negligible in the subsaturated regime (Bezantakos et al., 2016). For smaller particles and surface-active compounds, the surface tension may significantly affect the equilibrium water content.

3.3 Hygroscopicity of OS–AS mixture particles

We also examined the RH dependency of HGF for the studied OS–AS mixture particles at mass ratios (OS : AS) of 1 : 1, 1 : 3, and 1 : 5. Figure 3 shows the ZSR-predicted HGF as a function of RH for the three methyl sulfate (MS) salts mixed with AS. Whenever available, the corresponding experimental HGF data are presented as well. For other OS–AS mixture particles, the HGF data are presented in Fig. S7.

The estimated HGFs show that unlike the pure MS particles (dashed gray lines in Fig. 3), almost all the MS–AS mixture particles (solid lines) with the three chosen mass ratios exhibited gradual water uptake behaviors and then sharp deliquescence transitions at 60 % RH or above. With an increasing mass fraction of AS in the solute, the DRH of the MS–AS mixture particles shifts to higher RH but is still lower than the DRH of the pure AS (i.e., 80 % RH). The presence of AS noticeably lowered water uptake compared to the pure OS cases when RH was below the DRH. Similar results were observed in other OS–AS mixture particles (Fig. S7). However, when RH was above the DRH, the addition of AS only increases water uptake of KMS and other potassium OS particles.

Our HGF estimates are able to reproduce the measured HGF curves of the NaMS–AS mixture particles with a 1 : 1 mass ratio (Fig. 3a). For the NaMS–AS mixture particles with a 1 : 5 mass ratio, the HGF estimate well predicts the measurement data at RH $< 60\,\%$ or RH $> 80\,\%$, but there is disagreement around the DRH. A similar HGF underestimation at 60 %–80 % RH was also observed in NaHMS, NaHES, NaES, and NH_4HES mixture particles with AS with 1 : 3 and 1 : 5 mass ratios. For these 1 : 3 and 1 : 5 OS–AS mixture particles, the discrepancy between the measured and estimated HGFs is likely due to the underestimated interaction between OS and AS near the deliquescence phase transition and the resultant overestimated IAP of AS. It is also possible that solid AS partially dissolves into the liquid phase before the onset of deliquescence, thus leading to a higher HGF than expected at 60 %–80 % RH. Such partial disso-

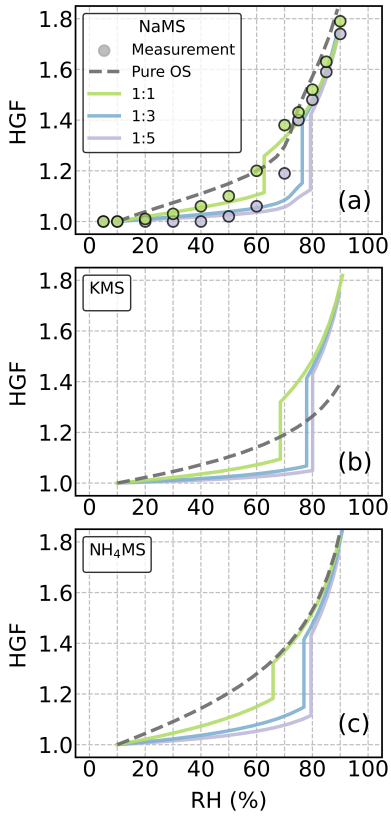

Figure 3. Hygroscopic growth factors (HGFs) of the mixture particles of ammonium sulfate (AS) and **(a)** sodium, **(b)** potassium, and **(c)** ammonium methyl sulfate as a function of RH at 295 K. The filled circles indicate measurement data from the literature (Peng et al., 2021). The HGF data derived from the COSMOtherm-based calculations are denoted by dashed lines for pure organosulfur (OS) compounds and by solid lines for the OS–AS mixed particles. Colors indicate different OS : AS mass ratios.

lution behavior of AS is not accounted for in our approach when the IAP of AS is below IAP_{sat}.

4 Conclusions

This novel approach does not require any reference OS data for optimization prior to HGF estimations. Instead, it is solely based on the quantum chemistry calculations and existing parameterizations of the commercially available COSMOtherm program. In this study, the COSMOtherm calculations show how the presence of sodium, potassium, and ammonium affects the α_w of OS. Given that these three cations originate from different emission sources in continental and marine environments, the α_w of OS can vary from one place to the next. Previous thermodynamic studies using COSMOtherm have provided α_w estimates consistent with those measured in bulk and particle phases for multifunctional atmospheric organics (Hyttinen et al., 2020b; Hyttinen and Prisle, 2020). As the first study modeling HGFs based on the COSMOtherm-estimated m_w, we show good agreement between COSMOtherm-derived and experimental HGFs in most cases of the studied OS. This highlights the potential applicability of COSMOtherm for estimating HGFs for other atmospheric compounds in future works.

Globally, SO_2 emissions are projected to decrease due to the phasing out of fossil fuels. This is expected to decrease the total and inorganic sulfur, thereby increasing the contribution of OS to total sulfur in atmospheric aerosol particles (Riva et al., 2019; Brüggemann et al., 2020). With progress in analytical instruments and methods, hundreds of OS compounds have been recently identified from field measurements (Hettiyadura et al., 2017, 2019; Wang et al., 2021; Huang et al., 2023; Wang et al., 2023; Yang et al., 2023). However, investigation of the physicochemical properties of OS is still lacking due to the scarcity of authentic standards. Our COSMOtherm-based approach allows the characterization of the hygroscopicity of OS particles even when authentic standards are unavailable. This will help us understand the aerosol–cloud–climate interactions in the post-fossil-fuel future where OS compounds will be highly important.

Data availability. The data set is available upon request from the corresponding author.

Supplement. The supplement related to this article is available online at: https://doi.org/10.5194/acp-24-11717-2024-supplement.

Author contributions. ZL and NH conceived the study. ZL performed the data collection and hygroscopicity calculation. NH performed the COSMOtherm calculations. ZL, AB, and NH analyzed and interpreted data. ZL wrote the paper with contributions from all coauthors.

Competing interests. The contact author has declared that none of the authors has any competing interests.

Disclaimer. Publisher's note: Copernicus Publications remains neutral with regard to jurisdictional claims made in the text, published maps, institutional affiliations, or any other geographical representation in this paper. While Copernicus Publications makes every effort to include appropriate place names, the final responsibility lies with the authors.

Acknowledgements. We thank Henry Oswin for the helpful discussion and CSC – IT Center for Science, Finland, for the computational resources.

Financial support. Zijun Li was supported by the QUT Early Career Research Scheme for funding support. Noora Hyttinen was supported by the Research Council of Finland (grant no. 338171) for the financial contribution.

Review statement. This paper was edited by Hailong Wang and reviewed by two anonymous referees.

References

Bain, A., Chan, M. N., and Bzdek, B. R.: Physical properties of short chain aqueous organosulfate aerosol, Environ. Sci. Atmos., 3, 1365–1373, https://doi.org/10.1039/D3EA00088E, 2023.

Barnes, I., Hjorth, J., and Mihalopoulos, N.: Dimethyl sulfide and dimethyl sulfoxide and their oxidation in the atmosphere, Chem. Rev., 106, 940–975, https://doi.org/10.1021/cr020529+, 2006.

Ben-Naim, A.: Solvation Thermodynamics, Plenum Press, New York and London, ISBN 978-1-4757-6552-6, 1987.

Berndt, T., Hoffmann, E. H., Tilgner, A., Stratmann, F., and Herrmann, H.: Direct sulfuric acid formation from the gas-phase oxidation of reduced-sulfur compounds, Nat. Commun., 14, 4849, https://doi.org/10.1038/s41467-023-40586-2, 2023.

Bezantakos, S., Huang, L., Barmpounis, K., Martin, S. T., and Biskos, G.: Relative humidity non-uniformities in hygroscopic tandem differential mobility analyzer measurements, J. Aerosol Sci., 101, 1–9, https://doi.org/10.1016/j.jaerosci.2016.07.004, 2016.

BIOVIA COSMOconf: Dassault Systèmes, http://www.3ds.com (last access: 29 January 2021), 2021.

BIOVIA COSMOtherm: Release 2021, Dassault Systèmes, http://www.3ds.com (last access: 1 April 2021), 2021.

Boyce, S. D. and Hoffmann, M. R.: Kinetics and mechanism of the formation of hydroxymethanesulfonic acid at low pH, J. Phys. Chem., 88, 4740–4746, https://doi.org/10.1021/j150664a059, 1984.

Brüggemann, M., Xu, R., Tilgner, A., Kwong, K. C., Mutzel, A., Poon, H. Y., Otto, T., Schaefer, T., Poulain, L., Chan, M. N., and Herrmann, H.: Organosulfates in ambient aerosol: state of knowledge and future research directions on formation, abundance, fate, and importance, Environ. Sci. Technol., 54, 3767–3782, https://doi.org/10.1021/acs.est.9b06751, 2020.

Campbell, J. R., Battaglia Jr, M., Dingilian, K., Cesler-Maloney, M., St Clair, J. M., Hanisco, T. F., Robinson, E., DeCarlo, P., Simpson, W., Nenes, A., Weber, R. J., and Mao, J.: Source and chemistry of hydroxymethanesulfonate (HMS) in Fairbanks, Alaska, Environ. Sci. Technol., 56, 7657–7667, https://doi.org/10.1021/acs.est.2c00410, 2022.

Chan, M. N., Lee, A. K., and Chan, C. K.: Responses of ammonium sulfate particles coated with glutaric acid to cyclic changes in relative humidity: Hygroscopicity and Raman characterization, Environ. Sci. Technol., 40, 6983–6989, 2006.

Choi, M. Y. and Chan, C. K.: The effects of organic species on the hygroscopic behaviors of inorganic aerosols, Environ. Sci. Technol., 36, 2422–2428, 2002.

Eckert, F. and Klamt, A.: Fast solvent screening via quantum chemistry: COSMO-RS approach, AIChE J., 48, 369–385, https://doi.org/10.1002/aic.690480220, 2002.

Estillore, A. D., Hettiyadura, A. P. S., Qin, Z., Leckrone, E., Wombacher, B., Humphry, T., Stone, E. A., and Grassian, V. H.: Water uptake and hygroscopic growth of organosulfate aerosol, Environ. Sci. Technol., 50, 4259–4268, https://doi.org/10.1021/acs.est.5b05014, 2016.

Glasius, M., Thomsen, D., Wang, K., Iversen, L. S., Duan, J., and Huang, R.-J.: Chemical characteristics and sources of organosulfates, organosulfonates, and carboxylic acids in aerosols in urban Xi'an, Northwest China, Sci. Total Environ., 810, 151187, https://doi.org/10.1016/j.scitotenv.2021.151187, 2022.

Hansen, A. M. K., Kristensen, K., Nguyen, Q. T., Zare, A., Cozzi, F., Nøjgaard, J. K., Skov, H., Brandt, J., Christensen, J. H., Ström, J., Tunved, P., Krejci, R., and Glasius, M.: Organosulfates and organic acids in Arctic aerosols: speciation, annual variation and concentration levels, Atmos. Chem. Phys., 14, 7807–7823, https://doi.org/10.5194/acp-14-7807-2014, 2014.

Hansen, A. M. K., Hong, J., Raatikainen, T., Kristensen, K., Ylisirniö, A., Virtanen, A., Petäjä, T., Glasius, M., and Prisle, N. L.: Hygroscopic properties and cloud condensation nuclei activation of limonene-derived organosulfates and their mixtures with ammonium sulfate, Atmos. Chem. Phys., 15, 14071–14089, https://doi.org/10.5194/acp-15-14071-2015, 2015.

Hettiyadura, A. P. S., Jayarathne, T., Baumann, K., Goldstein, A. H., de Gouw, J. A., Koss, A., Keutsch, F. N., Skog, K., and Stone, E. A.: Qualitative and quantitative analysis of atmospheric organosulfates in Centreville, Alabama, Atmos. Chem. Phys., 17, 1343–1359, https://doi.org/10.5194/acp-17-1343-2017, 2017.

Hettiyadura, A. P. S., Al-Naiema, I. M., Hughes, D. D., Fang, T., and Stone, E. A.: Organosulfates in Atlanta, Georgia: anthropogenic influences on biogenic secondary organic aerosol formation, Atmos. Chem. Phys., 19, 3191–3206, https://doi.org/10.5194/acp-19-3191-2019, 2019.

Hodas, N., Zuend, A., Schilling, K., Berkemeier, T., Shiraiwa, M., Flagan, R. C., and Seinfeld, J. H.: Discontinuities in hygroscopic growth below and above water saturation for laboratory surrogates of oligomers in organic atmospheric aerosols, Atmos. Chem. Phys., 16, 12767–12792, https://doi.org/10.5194/acp-16-12767-2016, 2016.

Hoffmann, E. H., Tilgner, A., Schrödner, R., Bräuer, P., Wolke, R., and Herrmann, H.: An advanced modeling study on the impacts and atmospheric implications of multiphase dimethyl sulfide chemistry, P. Natl. Acad. Sci. USA, 113, 11776–11781, https://doi.org/10.1073/pnas.1606320113, 2016.

Huang, D. D., Li, Y. J., Lee, B. P., and Chan, C. K.: Analysis of organic sulfur compounds in atmospheric aerosols at the HKUST supersite in Hong Kong using HR-ToF-AMS, Environ. Sci. Technol., 49, 3672–3679, https://doi.org/10.1021/es5056269, 2015.

Huang, L., Wang, Y., Zhao, Y., Hu, H., Yang, Y., Wang, Y., Yu, J.-Z., Chen, T., Cheng, Z., Li, C., Li, Z., and Xiao, H.: Biogenic and anthropogenic contributions to atmospheric organosulfates in a typical megacity in Eastern China, Geophys. Res. Atmos., 128, e2023JD038848, https://doi.org/10.1029/2023JD038848, 2023.

Hyttinen, N.: The effect of atmospherically relevant aminium salts on water uptake, Atmos. Chem. Phys., 23, 13809–13817, https://doi.org/10.5194/acp-23-13809-2023, 2023a.

Hyttinen, N.: Predicting liquid-liquid phase separation in ternary organic-organic-water mixtures, Phys. Chem. Chem. Phys., 25, 11121–11129, https://doi.org/10.1039/D3CP00691C, 2023b.

Hyttinen, N. and Prisle, N. L.: Improving solubility and activity estimates of multifunctional atmospheric organics by selecting conformers in COSMO*therm*, J. Phys. Chem. A, 124, 4801–4812, https://doi.org/10.1021/acs.jpca.0c04285, 2020.

Hyttinen, N., Elm, J., Malila, J., Calderón, S. M., and Prisle, N. L.: Thermodynamic properties of isoprene- and monoterpene-derived organosulfates estimated with COSMO*therm*, Atmos. Chem. Phys., 20, 5679–5696, https://doi.org/10.5194/acp-20-5679-2020, 2020a.

Hyttinen, N., Heshmatnezhad, R., Elm, J., Kurtén, T., and Prisle, N. L.: Technical note: Estimating aqueous solubilities and activity coefficients of mono- and α,ω-dicarboxylic acids using COSMO*therm*, Atmos. Chem. Phys., 20, 13131–13143, https://doi.org/10.5194/acp-20-13131-2020, 2020b.

Iinuma, Y., Müller, C., Berndt, T., Böge, O., Claeys, M., and Herrmann, H.: Evidence for the existence of organosulfates from β-pinene ozonolysis in ambient secondary organic aerosol, Environ. Sci. Technol., 41, 6678–6683, https://doi.org/10.1021/es070938t, 2007.

Jiang, H., Li, J., Tang, J., Cui, M., Zhao, S., Mo, Y., Tian, C., Zhang, X., Jiang, B., Liao, Y., Chen, Y., and Zhang, G.: Molecular characteristics, sources, and formation pathways of organosulfur compounds in ambient aerosol in Guangzhou, South China, Atmos. Chem. Phys., 22, 6919–6935, https://doi.org/10.5194/acp-22-6919-2022, 2022.

Klamt, A.: Conductor-like screening model for real solvents: a new approach to the quantitative calculation of solvation phenomena, J. Phys. Chem., 99, 2224–2235, https://doi.org/10.1021/j100007a062, 1995.

Klamt, A., Jonas, V., Bürger, T., and Lohrenz, J. C. W.: Refinement and parametrization of COSMO-RS, J. Phys. Chem. A, 102, 5074–5085, https://doi.org/10.1021/jp980017s, 1998.

Kristensen, K. and Glasius, M.: Organosulfates and oxidation products from biogenic hydrocarbons in fine aerosols from a forest in North West Europe during spring, Atmos. Environ., 45, 4546–4556, https://doi.org/10.1016/j.atmosenv.2011.05.063, 2011.

Kurtén, T., Hyttinen, N., D'Ambro, E. L., Thornton, J., and Prisle, N. L.: Estimating the saturation vapor pressures of isoprene oxidation products $C_5H_{12}O_6$ and $C_5H_{10}O_6$ using COSMO-RS, Atmos. Chem. Phys., 18, 17589–17600, https://doi.org/10.5194/acp-18-17589-2018, 2018.

Moch, J. M., Dovrou, E., Mickley, L. J., Keutsch, F. N., Liu, Z., Wang, Y., Dombek, T. L., Kuwata, M., Budisulistiorini, S. H., Yang, L., Decesari, S., Paglione, M., Alexander, B., Shao, J., Munger, J. W., and Jacob, D. J.: Global importance of hydroxymethanesulfonate in ambient particulate matter: Implications for air quality, Geophys. Res.-Atmos., 125, e2020JD032706, https://doi.org/10.1029/2020JD032706, 2020.

Ohno, P. E., Wang, J., Mahrt, F., Varelas, J. G., Aruffo, E., Ye, J., Qin, Y., Kiland, K. J., Bertram, A. K., Thomson, R. J., and Martin, S. T.: Gas-Particle Uptake and Hygroscopic Growth by Organosulfate Particles, ACS Earth Space Chem., 6, 2481–2490, https://doi.org/10.1021/acsearthspacechem.2c00195, 2022.

Pai, S. J., Heald, C. L., and Murphy, J. G.: Exploring the global importance of atmospheric ammonia oxidation, ACS Earth Space Chem., 5, 1674–1685, 2021.

Peng, C., Razafindrambinina, P. N., Malek, K. A., Chen, L., Wang, W., Huang, R.-J., Zhang, Y., Ding, X., Ge, M., Wang, X., Asa-Awuku, A. A., and Tang, M.: Interactions of organosulfates with water vapor under sub- and supersaturated conditions, Atmos. Chem. Phys., 21, 7135–7148, https://doi.org/10.5194/acp-21-7135-2021, 2021.

Peng, C., Malek, K. A., Rastogi, D., Zhang, Y., Wang, W., Ding, X., Asa-Awuku, A. A., Wang, X., and Tang, M.: Hygroscopicity and cloud condensation nucleation activities of hydroxyalkylsulfonates, Sci. Total Environ., 830, 154767, https://doi.org/10.1016/j.scitotenv.2022.154767, 2022.

Riva, M., Chen, Y., Zhang, Y., Lei, Z., Olson, N. E., Boyer, H. C., Narayan, S., Yee, L. D., Green, H. S., Cui, T., Zhang, Z., Baumann, K., Fort, M., Edgerton, E., Budisulistiorini, S. H., Rose, C. A., Ribeiro, I. O., e Oliveira, R. L., dos Santos, E. O., Machado, C. M. D., Szopa, S., Zhao, Y., Alves, E. G., de Sá, S. S., Hu, W., Knipping, E. M., Shaw, S. L., Duvoisin Junior, S., de Souza, R. A. F., Palm, B. B., Jimenez, J.-L., Glasius, M., Goldstein, A. H., Pye, H. O. T., Gold, A., Turpin, B. J., Vizuete, W., Martin, S. T., Thornton, J. A., Dutcher, C. S., Ault, A. P., and Surratt, J. D.: Increasing isoprene epoxydiol-to-inorganic sulfate aerosol ratio results in extensive conversion of inorganic sulfate to organosulfur forms: implications for aerosol physicochemical properties, Environ. Sci. Technol., 53, 8682–8694, https://doi.org/10.1021/acs.est.9b01019, 2019.

Robinson, R. A. and Stokes, R. H.: Electrolyte solutions, Courier Corporation, Courier Corporation, ISBN 978-0486422251, 2002.

Salter, M. E., Hamacher-Barth, E., Leck, C., Werner, J., Johnson, C. M., Riipinen, I., Nilsson, E. D., and Zieger, P.: Calcium enrichment in sea spray aerosol particles, Geophys. Res. Lett., 43, 8277–8285, 2016.

Song, S., Gao, M., Xu, W., Sun, Y., Worsnop, D. R., Jayne, J. T., Zhang, Y., Zhu, L., Li, M., Zhou, Z., Cheng, C., Lv, Y., Wang, Y., Peng, W., Xu, X., Lin, N., Wang, Y., Wang, S., Munger, J. W., Jacob, D. J., and McElroy, M. B.: Possible heterogeneous chemistry of hydroxymethanesulfonate (HMS) in northern China winter haze, Atmos. Chem. Phys., 19, 1357–1371, https://doi.org/10.5194/acp-19-1357-2019, 2019.

Stokes, R. H. and Robinson, R. A.: Interactions in aqueous nonelectrolyte solutions. I. Solute-solvent equilibria, J. Phys. Chem., 70, 2126–2131, https://doi.org/10.1021/j100879a010, 1966.

Surratt, J. D., Gómez-González, Y., Chan, A. W. H., Vermeylen, R., Shahgholi, M., Kleindienst, T. E., Edney, E. O., Offenberg, J. H., Lewandowski, M., Jaoui, M., Maenhaut, W., Claeys, M., Flagan, R. C., and Seinfeld, J. H.: Organosulfate formation in biogenic secondary organic aerosol, J. Phys. Chem. A, 112, 8345–8378, https://doi.org/10.1021/jp802310p, 2008.

Tolocka, M. P. and Turpin, B.: Contribution of organosulfur compounds to organic aerosol mass, Environ. Sci. Technol., 46, 7978–7983, https://doi.org/10.1021/es300651v, 2012.

TURBOMOLE: V7.5.1, a development of University of Karlsruhe and Forschungszentrum Karlsruhe GmbH, 1989–2007, TURBOMOLE GmbH, since 2007, https://www.turbomole.org (last access: 27 September 2022), 2020.

Vasilakopoulou, C. N., Matrali, A., Skyllakou, K., Georgopoulou, M., Aktypis, A., Florou, K., Kaltsonoudis, C., Siouti, E., Kostenidou, E., Błaziak, A., Nenes, A., Papagiannis, S., Eleftheriadis, K., Patoulias, D., Kioutsioukis, I., and Pandis, S. N.: Rapid transformation of wildfire emissions to harmful background aerosol, npj Climate and Atmospheric Science, 6, 218, https://doi.org/10.1038/s41612-023-00544-7, 2023.

Wang, Y., Zhao, Y., Wang, Y., Yu, J.-Z., Shao, J., Liu, P., Zhu, W., Cheng, Z., Li, Z., Yan, N., and Xiao, H.: Organosulfates in atmospheric aerosols in Shanghai, China: seasonal and interannual variability, origin, and formation mechanisms, Atmos. Chem. Phys., 21, 2959–2980, https://doi.org/10.5194/acp-21-2959-2021, 2021.

Wang, Y., Liang, S., Le Breton, M., Wang, Q. Q., Liu, Q., Ho, C. H., Kuang, B. Y., Wu, C., Hallquist, M., Tong, R., and Yu, J. Z.: Field observations of C_2 and C_3 organosulfates and insights into their formation mechanisms at a suburban site in Hong Kong, Sci. Total Environ., 904, 166851, https://doi.org/10.1016/j.scitotenv.2023.166851, 2023.

Wavefunction Inc.: Spartan'20, Irvine, CA, https://www.wavefun.com/spartan (last access: 1 October 2021), 2020.

Yang, T., Xu, Y., Ye, Q., Ma, Y.-J., Wang, Y.-C., Yu, J.-Z., Duan, Y.-S., Li, C.-X., Xiao, H.-W., Li, Z.-Y., Zhao, Y., and Xiao, H.-Y.: Spatial and diurnal variations of aerosol organosulfates in summertime Shanghai, China: potential influence of photochemical processes and anthropogenic sulfate pollution, Atmos. Chem. Phys., 23, 13433–13450, https://doi.org/10.5194/acp-23-13433-2023, 2023.

Ye, Y., Xie, Z., Zhu, M., and Wang, X.: Molecular Characterization of Organosulfates in Arctic Ocean and Antarctic atmospheric aerosols, Atmos. Chem. Phys. Discuss. [preprint], https://doi.org/10.5194/acp-2019-410, 2019.

Zhou, S., Guo, F., Chao, C.-Y., Yoon, S., Alvarez, S. L., Shrestha, S., Flynn III, J. H., Usenko, S., Sheesley, R. J., and Griffin, R. J.: Marine submicron aerosols from the Gulf of Mexico: Polluted and acidic with rapid production of sulfate and organosulfates, Environ. Sci. Technol., 57, 5149–5159, https://doi.org/10.1021/acs.est.2c05469, 2023.

Zuend, A. and Seinfeld, J. H.: Modeling the gas-particle partitioning of secondary organic aerosol: the importance of liquid-liquid phase separation, Atmos. Chem. Phys., 12, 3857–3882, https://doi.org/10.5194/acp-12-3857-2012, 2012.

Zuend, A., Marcolli, C., Luo, B. P., and Peter, T.: A thermodynamic model of mixed organic-inorganic aerosols to predict activity coefficients, Atmos. Chem. Phys., 8, 4559–4593, https://doi.org/10.5194/acp-8-4559-2008, 2008.

Zuend, A., Marcolli, C., Booth, A. M., Lienhard, D. M., Soonsin, V., Krieger, U. K., Topping, D. O., McFiggans, G., Peter, T., and Seinfeld, J. H.: New and extended parameterization of the thermodynamic model AIOMFAC: calculation of activity coefficients for organic-inorganic mixtures containing carboxyl, hydroxyl, carbonyl, ether, ester, alkenyl, alkyl, and aromatic functional groups, Atmos. Chem. Phys., 11, 9155–9206, https://doi.org/10.5194/acp-11-9155-2011, 2011.